Development 139, 1359-1367 (2012) doi:10.1242/dev.072371

Vimentin regulates peripheral nerve myelination

Daniela Triolo[1,2], Giorgia Dina[1,2], Carla Taveggia[1,2], Ilaria Vaccari[1,2,3], Emanuela Porrello[1,2], Cristina Rivellini[1,2], Teuta Domi[1,2], Rosa La Marca[1,2], Federica Cerri[1,2,4], Alessandra Bolino[1,2,3], Angelo Quattrini[1,2,4] and Stefano Carlo Previtali[1,2,4,*]

SUMMARY

Myelination is a complex process that requires coordinated Schwann cell-axon interactions during development and regeneration. Positive and negative regulators of myelination have been recently described, and can belong either to Schwann cells or neurons. Vimentin is a fibrous component present in both Schwann cell and neuron cytoskeleton, the expression of which is timely and spatially regulated during development and regeneration. We now report that vimentin negatively regulates myelination, as loss of vimentin results in peripheral nerve hypermyelination, owing to increased myelin thickness in vivo, in transgenic mice and in vitro in a myelinating co-culture system. We also show that this is due to a neuron-autonomous increase in the levels of axonal neuregulin 1 (NRG1) type III. Accordingly, genetic reduction of NRG1 type III in vimentin-null mice rescues hypermyelination. Finally, we demonstrate that vimentin acts synergistically with TACE, a negative regulator of NRG1 type III activity, as shown by hypermyelination of double *Vim*/*Tace* heterozygous mice. Our results reveal a novel role for the intermediate filament vimentin in myelination, and indicate vimentin as a regulator of NRG1 type III function.

KEY WORDS: Myelination, Cytoskeleton, Neuregulin 1 type III, TACE, Mouse

INTRODUCTION

Myelination in the nervous system is essential for rapid and efficient propagation of action potentials. Myelin sheath thickness and compaction are affected in numerous peripheral neuropathies (Suter and Scherer, 2003), indicating that controlled growth of the myelin sheath is crucial during myelination and myelin maintenance. Nevertheless, the basic molecular mechanisms controlling myelin thickness are only partially understood. The key molecule regulating myelin formation in the peripheral nervous system (PNS) is neuregulin 1 type III (NRG1), the activity of which is regulated by extracellular cleavage (Michailov et al., 2004; Taveggia et al., 2005). This cleavage is mediated by positive and negative regulators such as BACE1 (Hu et al., 2006; Willem et al., 2006) and TACE (ADAM17 – Mouse Genome Informatics) secretases (La Marca et al., 2011).

Intermediate filaments (IFs) constitute a large family of proteins expressed with a tissue-specific and spatial-temporal pattern in mammals (Coulombe and Wong, 2004; Eriksson et al., 2009). In addition to being involved in nerve development and regeneration, IFs, the third fibrous component of the cytoskeleton besides microtubules and microfilaments, may also play a prominent role in myelination. In the peripheral nerve, Schwann cells express glial fibrillary acidic protein (GFAP) in development and nerve regeneration, whereas in the adult nerves GFAP expression is restricted to non-myelin forming Schwann cells (Jessen and Mirsky, 1991; Jessen and Mirsky, 2005). Axons express neurofilaments and peripherin, which are associated to the maintenance of axonal caliber (Julien, 1999), and to axonal sprouting, respectively (Belecky-Adams et al., 2003). Vimentin is an IF that is abundantly expressed in both Schwann cells and neurons. Its expression is high during embryonic development, whereas postnatal vimentin expression is restricted to myelin-forming Schwann cells (Jessen and Mirsky, 1991; Neuberger and Cornbrooks, 1989), and is gradually replaced by neurofilaments in neurons (Cochard and Paulin, 1984; Perlson et al., 2005). Of note, vimentin expression is rapidly upregulated in Schwann cells and neurons during nerve regeneration. Recently, axonal vimentin has been implicated in nerve regeneration (Perlson et al., 2005). However, whether vimentin plays a role in peripheral nerve function and myelination still remains to be determined.

We now report that vimentin is required for proper PNS myelination. Loss of neuronal vimentin induces increased myelin sheath thickness by controlling levels of axonal NRG1 type III. Accordingly, rescue experiments aimed at reducing levels of NRG1 type III in vimentin-null nerves resulted in normal myelination. Finally, vimentin and TACE genetically interact to regulate NRG1 type III levels, as double heterozygous mice ($Vim^{+/-}$ $Tace^{+/-}$) are hypermyelinated.

MATERIALS AND METHODS

Mice

Generation of vimentin-null ($Vim^{-/-}$), $Nrg1^{+/-}$ and $Tace^{+/-}$ mice has been previously reported (Colucci-Guyon et al., 1994; Horiuchi et al., 2007; McCall et al., 1996; Wolpowitz et al., 2000). The mouse colonies used in our experiments are congenic in C57/Bl6 background. All animal procedures were carried out following Italian regulations and in accordance with the S. Raffaele Institutional Animal Care and Use Committee.

Mouse and rat DRG co-cultures

Mouse DRGs were isolated from E13.5 embryos and organotypic co-cultures were established as described (Bolis et al., 2009; Taveggia et al., 2005). For purified DRG neurons co-cultured with wild-type rat Schwann cells, mouse DRGs were first incubated with trypsin (0.25%) for 45 minutes at 37°C, then mechanically dissociated and plated at a concentration of one to two DRGs per glass coverslip. Isolated rat Schwann cells were prepared as reported previously (Taveggia et al., 2005) and cultured using DMEM with 10% of fetal calf serum, 2 ng/ml recombinant human neuregulin1-β1 (R&D Systems) and 2 μM forskolin (Calbiochem).

[1]Institute of Experimental Neurology (INSPE) , San Raffaele Scientific Institute, Via Olgettina 60, 20132 Milan, Italy. [2]Division of Neuroscience, San Raffaele Scientific Institute, Via Olgettina 60, 20132 Milan, Italy. [3]Dulbecco Telethon Institute, San Raffaele Scientific Institute, Via Olgettina 60, 20132 Milan, Italy. [4]Department of Neurology, San Raffaele Scientific Institute, Via Olgettina 60, 20132 Milan, Italy.

*Author for correspondence (previtali.stefano@hsr.it)

Accepted 18 January 2012

Histology and morphometric analysis

Semi-thin and ultra-thin morphological studies were performed as described previously (Previtali et al., 2000), and examined by light (Olympus BX51, Segrate, Italy) and electron microscopy (Zeiss CEM 902, Arese, Italy). Digitalized images of fiber cross-sections were obtained from corresponding levels of the sciatic nerve with a digital camera (Leica DFC300F, Milano, Italy) using a 100× objective. At least four images from four different animals per genotype were acquired (25×10^3 μm^2 of sciatic nerve per each animal). Morphometry on semi-thin sections was analyzed with the Leica QWin software (Leica Mycrosystems, Milano, Italy) (Triolo et al., 2006). The ratio between the mean diameter of an axon and the mean diameter of the fiber, including myelin (g-ratio), was determined on at least 300 randomly chosen fibers per genotype (three animals per genotype).

Antibodies

Antibodies used for immunohistochemistry/western blotting were: anti-actin (Sigma, St Louis, MO, USA); total AKT and phosphorylated AKT (Cell Signaling, Danvers, MA); erbB2 and phosphorylated erbB2 (Santa Cruz Biotechnology, Santa Cruz, CA); myelin basic protein (MBP; Millipore, Vimodrone, Italy); β-tubulin (TUB 2.1, Sigma); calnexin (Sigma); GFAP (GA5, Millipore); Krox20 (Covance); total p44-p42 MAP kinases, p-p44 and p-p42 (Cell Signaling); myelin-associated glycoprotein (MAG; Millipore); neurofilament-H (Millipore); neurofilament-L (NR4, Sigma); neurofilament-M (Covance); Peripherin (Millipore); protein-P0 (Abcam, Cambridge, MA); S100 (Sigma); and vimentin (LN6, Sigma; rabbit, Millipore).

Immunohistochemistry

Immunofluorescence on cryosections was performed as described previously (Triolo et al., 2006), and examined with confocal (Leica SP5, Leica Mycrosystems) and fluorescent microscopes (Olympus BX51, Segrate, Italy). The erbB2/B3-Fc fusion protein was obtained as described (Taveggia et al., 2005). Unfixed neurons were incubated with the supernatant containing erbB2/B3-Fc for 2 hours at 37°C, and then fixed and revealed with anti-human Fc antibody (Jackson Laboratories, Bar Arbor, ME). The amount of fluorescence was calculated using ImageJ over an area of 5 fields/cover and normalized for the background.

Analysis of myelination

Myelination in DRG explants was evaluated as follows: using a fluorescence microscope (Olympus BX51) at least 5 fields/cover were randomly acquired near to sensory neurons, where usually myelination is more efficient and abundant. The percentage of MBP-positive fibers among the total number of MBP-positive fibers was indicated. This method was validated by scoring MBP-positive myelinated fibers on random fields after 7 days of ascorbic acid treatment and the results were absolutely consistent. Myelination in dissociated Schwann cell/DRG neuron co-cultures was similarly evaluated: at least 10 fields/cover were randomly acquired and MBP-positive segments and Schwann cell nuclei were counted per field. Results were expressed as a ratio between MBP-positive segments and the Schwann cell nuclei.

Western blotting

Proteins were isolated from snap-frozen sciatic nerves of mice and western blotting performed as described (Triolo et al., 2006). Briefly, nerves were suspended in Tris-buffered SDS or Triton X-100 lysis buffer, sonicated and boiled. Equal amounts of homogenates (5 μg for myelin proteins, 50 μg for erbB2 and 10-20 μg for other proteins) were separated in Laemli sample buffer on SDS-PAGE gel and transferred to nitrocellulose membrane (Biorad, Segrate, Italy). Blots were blocked in PBS/0.05% Tween 20/5% dried milk or BSA, incubated with the appropriate primary and peroxidase-conjugated secondary antibody visualized by ECL (Amersham, Cologno M., Italy), or with a fluorophore-conjugated secondary antibody visualized using Odissey Imaging System (LI-COR Biosciences, Lincoln, NE, USA).

shRNA and lentiviral (LV) production

To downregulate expression of vimentin in isolated Schwann cells, two different shRNA clones were used (Open Biosystems; TRCN0000089832 and TRCN0000029122) cloned into the pLKO.1 LV (human U6 promoter), without a GFP reporter. The transfer constructs were transfected into 293FT cells together with packaging plasmids –8.9 and pCMV-VSGV using Lipofectamine 2000 (Invitrogen). As a control, a vector encoding an shRNA to a nonspecific sequence (luciferase+GFP) was used. Viral supernatants were collected 72 hours after transfection, centrifuged at 3000 rpm for 15 minutes and frozen at –80°C. Using non-concentrated LV, transduction of Schwann cells was performed in two consecutive overnights. After 48 hours from infection, cells were harvested and plated on dissociated wild-type mouse DRGs at 200,000 cells/coverslip. Myelination was induced after 2 days from the seeding by using C-media and ascorbic acid for 7 days. To assess vimentin downregulation in isolated Schwann cells, cells were cultured for 7-10 days after LV transduction and analyzed by western blot.

Statistical analyses

Statistical analyses were evaluated by two tail Student's *t*-test in all the experiments, except for the analysis of % of axons in Remak bundles and in Schwann cell pocket in which we used χ^2 test.

RESULTS

To assess loss of vimentin expression in vimentin-null (*Vim*$^{-/-}$) mouse nerves, we stained mutant and control nerve sections using anti-vimentin antibody at P15 and P60. Vimentin-null nerves did not show vimentin staining in either Schwann cells or axons (Fig. 1C,D,F), confirming successful targeted mutagenesis in peripheral

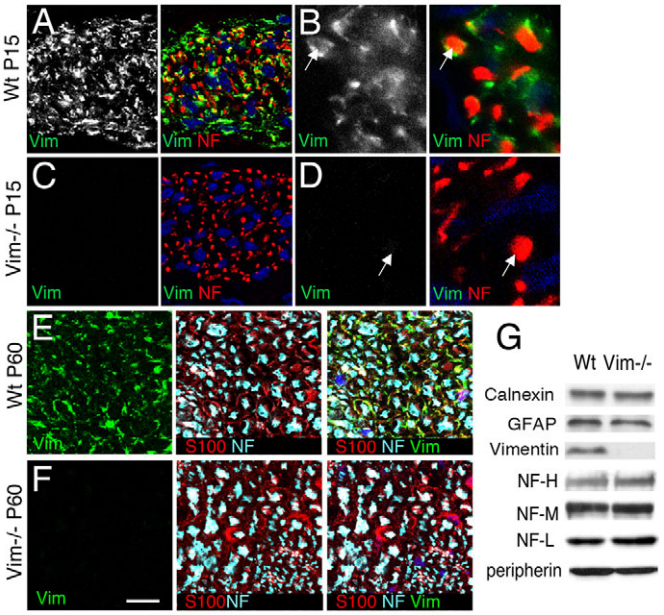

Fig. 1. Loss of vimentin in the peripheral nerve. (**A-D**) Staining for neurofilament (red) and vimentin (green) in P15 sciatic nerves of wild-type (A,B) and vimentin-null (C,D) mice. Vimentin staining is absent in the mutant mouse (C,D). When overexposed, vimentin signal is evident not only in myelinating Schwann cells, but also in some axons (note yellow signal in A, indicating colocalization of vimentin and neurofilament signal; and faint fluorescence in B, when image is highly magnified, see arrows). Even when overexposed, we could not detect any signal for vimentin in null mice (C,D; see arrows). (**E**,**F**) Staining for vimentin (green), S100 (red) and neurofilaments (light blue) in P60 sciatic nerves of wild-type (E) and vimentin-null (F) mice. Vimentin staining is primarily in myelin-forming Schwann cells (identified by S100, yellow signal in merge image), and absent in vimentin-null nerves. Dark blue identifies nuclei by DAPI staining. (**G**) Western blot analysis confirms that vimentin is absent in sciatic nerve homogenate from adult mutant mice, whereas the amount of other intermediate filaments in Schwann cells and axons is similar to control. Scale bar: 60 μm in A,C; 6 μm in B,D; 30 μm in E,F.

nerves. Interestingly, in control nerves, besides the expected staining in myelin-forming Schwann cells more evident in P60 nerves (yellow signal in Fig. 1E), some axon showed vimentin reactivity when the signal was overexposed (yellow signal in Fig. 1A, arrow in 1B). Moreover, loss of vimentin did not result in any compensatory expression of other known intermediate filaments in Schwann cells and axons. Western blotting for GFAP, peripherin, neurofilament-L, neurofilament-M and neurofilament-H showed similar amount in sciatic nerve homogenate of adult vimentin-null and wild-type mice (Fig. 1G).

Vimentin-null mice are hypermyelinated

We then analyzed the morphology of peripheral nerves of adult mice (P60). We did not find differences in total fiber number and fiber type distribution in sciatic nerves of vimentin-null when compared with wild-type mice (Fig. 2A-C). Surprisingly, the myelin sheath of most vimentin-null fibers was thicker than control fibers (Fig. 2B-D). Consistently, the mean g-ratio (the ratio between the diameter of an axon and the diameter of the fiber including myelin) of vimentin-null fibers was significantly reduced when compared with controls (wild type 0.70±0.002 versus $Vim^{-/-}$ 0.67±0.002; $P<0.001$; $n=600$ fibers per genotype, three mice per genotype). When we analyzed g-ratio within classes of fibers binned for their axonal diameter, increased myelin thickness was present for all diameters (Fig. 2E). As hypermyelination could result by pathological shrinkage of the axonal caliber, we evaluated axon size distribution and we did not find any difference between vimentin-null and control mice (data not shown), suggesting that hypermyelination was due to an increased number of myelin lamellae.

Length of internodal Schwann cells is directly proportional to axon diameter and myelin thickness (Friede and Bischhausen, 1980). Thus, we evaluated whether internodal length was changed in vimentin-null nerves. In agreement with thicker myelin sheath, we found that internodal lengths were significantly longer in vimentin-null mice than in controls (wild type 678±5 μm versus $Vim^{-/-}$ 735±7 μm; $P=0.003$; $n=70$ fibers per mouse, three mice per genotype).

We then evaluated whether hypermyelination was present at earlier time points, during development. We analyzed sciatic nerves at P20, when myelination is actively ongoing and we observed fibers with increased myelin thickness and significantly reduced g-ratio in vimentin-null mice (wild type 0.69±0.003 versus $Vim^{-/-}$ 0.64±0.003; $P<0.001$; $n=300$ fibers per genotype, three mice per genotype). We also evaluated whether the timing of myelination was anticipated in vimentin-null nerves. Ultrastructural analysis of vimentin-null sciatic nerves at P1 showed that the onset of myelination was similar to controls (wild type 1.8±0.3 versus $Vim^{-/-}$ 1.5±0.3 myelinated fibers per 200 μm^2; P value is not significant; $n=3$ mice per genotype; Fig. 2F).

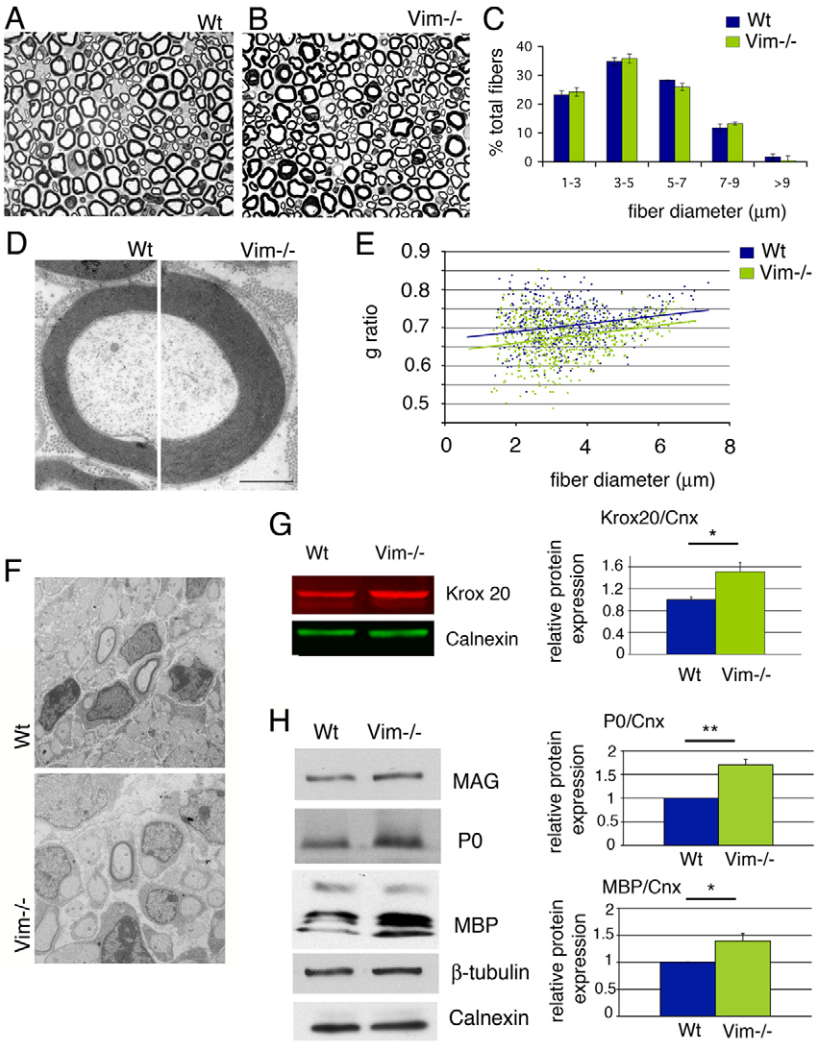

Fig. 2. Vimentin-null nerves are hypermyelinated. (**A**,**B**) Semi-thin sections of sciatic nerve from 2-month-old wild-type (A) and vimentin-null (B) mice. Vimentin-null mice show several fibers with increased myelin thickness. (**C**) Morphometric analysis did not show significant differences in terms of fiber size and density between wild-type and vimentin-null mice. (**D**) Electron micrograph depicting a single sciatic nerve fiber hypermyelinated in adult vimentin-null mouse (right) when compared with an axon of similar diameter in wild-type mouse (left). (**E**) g-ratio is consistently reduced in vimentin-null nerves (green) when compared with wild type (blue) for virtually all axon diameters. (**F**) Semi-thin section of sciatic nerve from P1 wild-type and vimentin-null mice. Few myelinated fibers are present in both genotypes without significant differences. (**G**) Sciatic nerve homogenates from P5 wild-type and vimentin-null mice, blotted with anti-KROX20 antibody and calnexin as a loading control, and revealed for quantification using the Odissey Imaging System. Quantification of western blot analysis is reported as an average of three independent experiments, and represented as ratio KROX20/calnexin, assigning wild type as 1±s.e.m. KROX20 levels were significantly increased in vimentin-null nerves when compared with wild type (*$P=0.04$; $n=3$). (**H**) Sciatic nerve homogenates from P20 wild-type and vimentin-null mice blotted with anti-myelin proteins (P0 and MBP), myelin-associated glycoprotein (MAG) and calnexin for loading control. Quantification of western blot analysis is reported as an average of three independent experiments, and represented as the ratios P0/calnexin and MBP/calnexin, assigning wild type as 1±s.e.m. A significant increased amount of P0 (**$P=0.004$; $n=3$) and MBP (*$P=0.04$; $n=3$) was observed in the vimentin-null homogenate. Scale bar: 18 μm in A,B; 1.4 μm in D; 2.5 μm in F.

Western blotting analyses for the promyelinating transcription factor KROX20 (EGR2 – Mouse Genome Informatics) and myelin proteins further confirmed hypermyelination in vimentin-null nerves. At P5, KROX20 was significantly increased in vimentin-null nerves when compared with wild type (Fig. 2G). Similarly, the expression of MBP and P0 (myelin protein zero), the major peripheral myelin proteins, were also significantly increased in vimentin-null when compared with wild-type mice during active myelination (P20; Fig. 2H) and in adult mice (P60; data not shown). Overall, our data suggest that hypermyelination in vimentin-null mice is a developmental process and not a transient phenomenon.

Vimentin hypermyelination is neuronal dependent

As vimentin is expressed in both Schwann cells and neurons in the peripheral nerves (Cochard and Paulin, 1984; Perlson et al., 2005) (Fig. 1), we sought to determine whether the hypermyelination was due to a Schwann cell 'intrinsic' or 'extrinsic' mechanism. Thus, we moved to an in vitro myelinating system by co-culturing Schwann cells with DRG sensory neurons.

First, we determined whether vimentin-null Schwann cell/DRG neuronal co-culture reproduced the hypermyelinating phenotype observed in vivo in vimentin-null mice. Vimentin-null and wild-type E13.5 organotypic DRG explants showed similar extent of neurite outgrowth, as measured 7 days after plating (wild type 5.10±0.23 mm versus $Vim^{-/-}$ 5.10±0.10 mm; n=12; P value is not significant; data not shown). We then induced myelination by supplementing the cultures with 50 μg/ml of ascorbic acid. Seven days after addition of 50 μg/ml ascorbic acid, immunofluorescence analysis for MBP segments showed increased myelination in vimentin-null co-cultures. The number of MBP-positive segments was in fact significantly increased in vimentin-null co-cultures when compared with controls (wild type 101±16/mm^2 versus $Vim^{-/-}$ 255±42/mm^2; P=0.002; n=33 per genotype; Fig. 3A-C). Furthermore, ultrastructural analyses showed that both vimentin-null and wild-type co-cultures had normal compact myelin sheath, and confirmed that myelin was thicker in vimentin-null DRGs (Fig. 3D,E; at 14 days after ascorbic acid, g-ratio: wild type 0.75±0.009 versus $Vim^{-/-}$ 0.72±0.01; P=0.02; n=40 per genotype).

To determine the cell autonomy of hypermyelination, we co-cultured dissociated mouse DRG neurons from vimentin-null mice, which are devoid of endogenous Schwann cells, together with isolated wild-type rat Schwann cells. Myelination in co-cultures lacking neuronal vimentin, was significantly increased when compared with wild-type control cultures (respectively 282.3±2.1 MBP-positive segments/mm^2 versus 130.7±1.9 MBP-positive segments/mm^2; n=20 coverslips per genotype; P<0.001; Fig. 3F-H). Thus, the lack of neuronal vimentin is sufficient to induce hypermyelination.

To evaluate whether loss of vimentin in Schwann cells may also contribute to the hypermyelinating phenotype, we performed the reverse experiment. We knocked down vimentin expression in rat Schwann cells by using specific *Vim* shRNA encoding lentiviruses and co-cultured them with wild-type DRG neurons. Western blot analysis showed that vimentin expression in transduced rat Schwann cells was reduced up to 90% (Fig. 3M). As a control, rat Schwann cells were transduced with scramble shRNA. Myelination was not upregulated in co-cultures with knocked down Schwann cells, when compared with wild-type or scramble-infected Schwann cells (Fig. 3I-L). This result confirmed that hypermyelination in vimentin-null mice is due to loss of vimentin

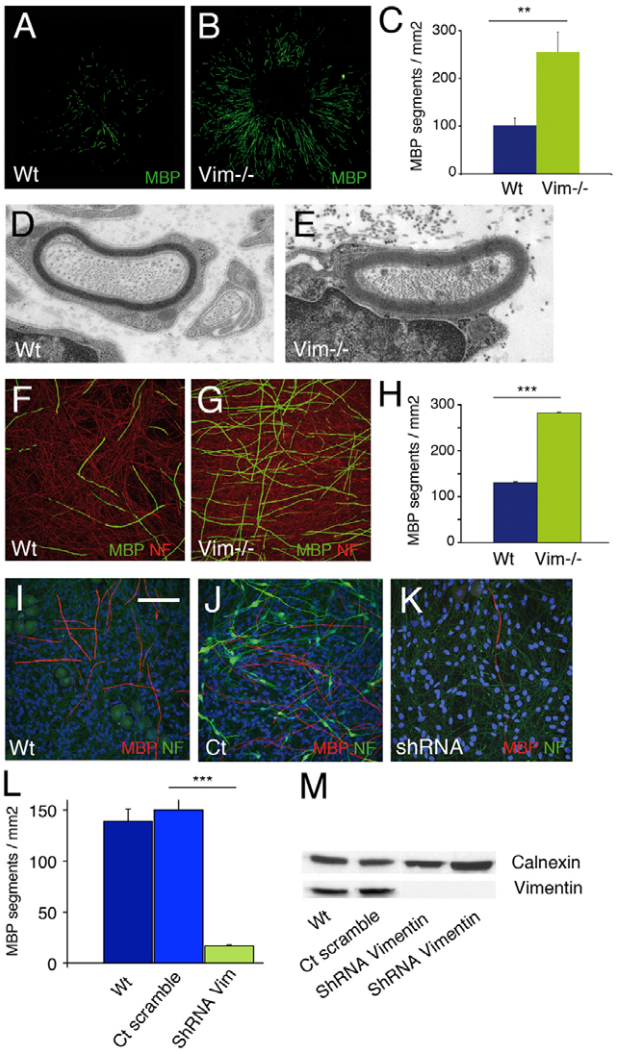

Fig. 3. Hypermyelination in vimentin-null nerves is neuronal intrinsic. (**A-C**) Reconstruction of an entire DRG explant from wild-type (A) and vimentin-null (B) mouse embryo at E13.5, and stained for MBP (green) and neurofilament (red) 7 days after ascorbic acid treatment. The number of myelinated segments were significantly increased in vimentin-null DRG explants (C), $**P$<0.01. (**D**,**E**) Electron micrographs of DRG explant from wild-type (D) and vimentin-null (E) mouse embryo 14 days after ascorbic acid treatment. Vimentin-null fibers showed increased myelin thickness. (**F-H**) Rat Schwann cells were seeded in vitro on mouse sensory neurons from wild-type (F) and vimentin-null (G) mice. Co-cultures were stained for MBP (green) and neurofilament (red) 7 days after ascorbic acid treatment. The number of myelinated segments was significantly increased in co-cultures of vimentin-null neurons (H), $***P$<0.001. (**I-M**) Wild-type mouse sensory neurons devoid of fibroblasts and Schwann cells were co-cultured with wild-type rat Schwann cells (I); wild-type rat Schwann cells transduced with scramble shRNA LV as control (J), and wild-type rat Schwann cells transduced with *Vim* ShRNA LV (K) to obtain vimentin-null Schwann cells. (L) The number of myelinated segments was similar in co-cultures with wild type (Wt) Schwann cells and Schwann cells transduced with scramble shRNA LV (Ct scramble), whereas the number was significantly reduced in co-cultures with Schwann cells transduced using *Vim* ShRNA LV, $***P$<0.001. (M) Efficacy of vimentin downregulation was demonstrated by western blot analysis, which shows absence of vimentin in Schwann cell lysate. Co-cultures were stained for MBP and neurofilament 7 days after ascorbic acid treatment. Each experiment (A-C,F-H,I-M) was performed at least three times. Scale bar: 2.3 mm in A,B; 0.5 μm in D,E; 100 μm in F,G,I-K.

in neurons and not in Schwann cells. Surprisingly, vimentin-null Schwann cells co-cultured with wild-type neurons yielded a reduced number of myelinated segments when compared with controls (respectively 17±1/mm^2 versus 150±19.6/mm^2; P<0.0001; n=12 coverslips per genotype; Fig. 3I-L). Although the number of Schwann cells in co-culture with shRNA for vimentin was 50% reduced when compared with scramble-infected co-cultures (2000 Schwann cells/mm^2 versus 4000/mm^2), the overall number of MBP-positive segments were reduced to one-tenth. Thus, reduced myelination is not likely to be a consequence in the reduced Schwann cell number but an intrinsic defect in glial cells. This experiment may reveal an additional role of vimentin during Schwann cell development, which is likely masked in vivo by the presence of other intermediate filaments. Overall, these data suggest that hypermyelination in vimentin-null mice is due to a neuronal intrinsic mechanism.

Loss of vimentin in neurons determines increased expression of NRG1 type III and hypermyelination

Previous studies showed that threshold levels of axonal NRG1 type III, signaling via activation of the erbB2/3 receptor in Schwann cells, determines the ensheathment fate of the axons and the amount of myelin formed (Michailov et al., 2004; Taveggia et al., 2005). As the hypermyelination in vimentin-null mice was primarily neuronal intrinsic, we investigated whether thicker myelin was due to increased levels of NRG1 type III. DRG neurons from wild-type and vimentin-null mice were incubated with ERBB2/3-Fc (Fitzpatrick et al., 1998), a chimeric protein containing the extracellular region of the ERBB2 and ERBB3-NRG1 receptors fused to the Fc region of human IgG. This molecule binds with high affinity to axonal NRG1 type III (Taveggia et al., 2005). Chimeric ERBB2/3-Fc bound more robustly to vimentin-null neurons when compared with wild-type neurons (Fig. 4A,B). This result was further confirmed by western blot analysis, showing that levels of NRG1 were significantly increased in isolated DRG neurons from vimentin-null mice when compared with controls (Fig. 4C).

As PI-3K is a key effector of NRG1 type III signaling and myelination (Ogata et al., 2004), we evaluated whether this pathway was modulated in vimentin-null nerves. Consistent with higher levels of NRG1 type III in neurons, we found that levels of phosphorylated Akt were significantly increased in vimentin-null nerves at P20 (P=0.02) and in adult (P60) mice (P=0.0004). Levels of phosphorylated p44 and p42 (MAPK) did not change significantly (Fig. 5 and data not shown). Finally, we evaluated levels of phosphorylated ERBB2 receptors, which heterodimerize with ERBB3 to constitute the active form of NRG1 receptor in Schwann cells. Levels of phospho-ERBB2 were significantly increased at P20 in vimentin-null when compared with wild-type nerves (P=0.02, n=3; Fig. 5B). Taken together, these results provide evidence that hypermyelination in vimentin-null mice is the consequence of increased NRG1 type III level.

Decreased levels of NRG1 type III rescues hypermyelination in vimentin-null mice

To finally prove that hypermyelination in vimentin-null mice is due to increased levels of NRG1 type III, we downregulated *Nrg1* by crossing vimentin-null mice with hypomyelinated *Nrg1*$^{+/-}$ mice (Taveggia et al., 2005). As expected, adult *Vim*$^{-/-}$ *Nrg1*$^{+/-}$ mice showed reduced myelin thickness in sciatic nerve when compared with *Vim*$^{-/-}$ *Nrg1*$^{+/+}$ mice (Fig. 6A-D). Mean g-ratio in *Vim*$^{-/-}$ *Nrg1*$^{+/-}$ mice was significantly increased when compared with

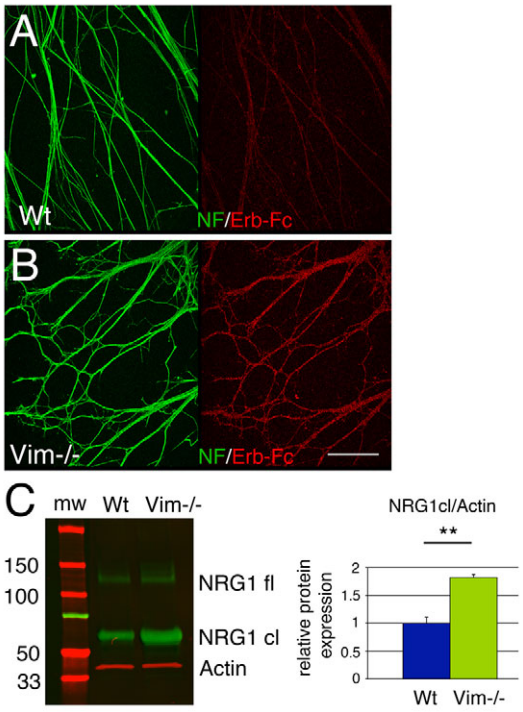

Fig. 4. Vimentin-null neurons have increased levels of type III NRG1. (**A**,**B**) Co-cultures of wild-type (A) and vimentin-null (B) sensory neurons were stained with ERBB2/3-Fc (red) and neurofilament (green) antibody 7 days after ascorbic acid treatment. Increased binding of ERBB2/3-Fc to vimentin-null when compared with wild-type neurons was observed. Images have been acquired by confocal microscope with the same *z*-stack and laser intensity. (**C**) Lysates of sensory neurons from wild-type and vimentin-null mice were blotted with ERBB2/3-Fc. The antibody recognized the 135 kDa band corresponding to the full-length NRG1 (NRG1-fl) pro-protein and the active cleaved fragment of NRG1 (NRG1-cl). Actin was used as a loading control. The active NRG1-cl was significantly increased in vimentin-null mice. Quantification of western blot analysis is reported as an average of three independent experiments and represented as ratio NRG1cl/actin, assigning wild type as 1±s.e.m., **P=0.002. Scale bar: 110 μm in A,B.

Vim$^{-/-}$ *Nrg1*$^{+/+}$ mice (0.74±0.0007 versus 0.67±0.0008, respectively; P<0.001; n=300 fibers per genotype, four mice per genotype).

Western blot analysis for myelin proteins (P0 and MBP) and phosphorylated Akt levels confirmed that 50% reduction of NRG1 type III is sufficient to rescue hypermyelination. In fact, P0 and MBP protein levels (Fig. 6E) and phospho-Akt (Fig. 6F), which are increased in *Vim*$^{-/-}$ nerves, were reduced to normal levels in *Vim*$^{-/-}$ *Nrg1*$^{+/-}$ mice.

If loss of vimentin increases NRG1 type III levels, morphological defects observed in *Nrg1*$^{+/-}$ nerves should be rescued (or ameliorated) in *Nrg1*$^{+/-}$ mice when vimentin is also lost (*Vim*$^{-/-}$ *Nrg1*$^{+/-}$). Thus, to further demonstrate that vimentin modulates NRG1 type III levels, we analyzed Remak bundles in *Nrg1*$^{+/-}$ mice, which are abnormally organized as a consequence of reduced NRG1 type III levels. In *Nrg1*$^{+/-}$, non-myelin forming Schwann cells are associated with an increased number of axons, and these axons are frequently incompletely segregated into Schwann cell pockets (Taveggia et al., 2005). Accordingly, abnormal axonal segregation observed in *Nrg1*$^{+/-}$ mice is ameliorated in sciatic nerves of *Vim*$^{-/-}$ *Nrg1*$^{+/-}$, as loss of vimentin

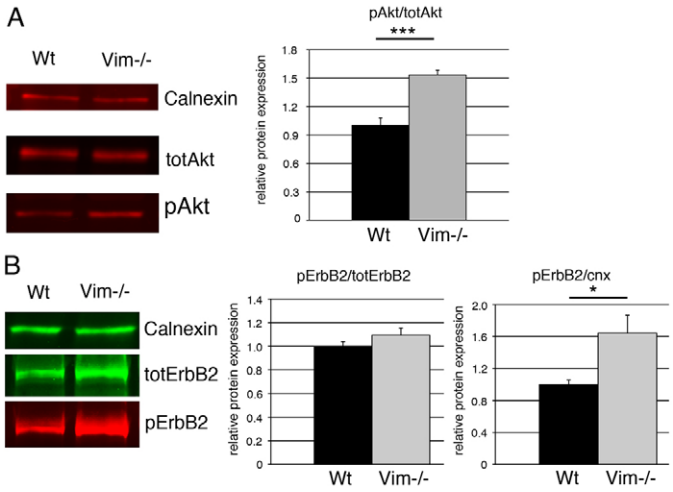

Fig. 5. Vimentin-null nerves have increased levels of pAkt. (**A**) Homogenate of sciatic nerve lysates from P60 wild-type and vimentin-null mice. Blots were probed for phospho-Akt (pAkt), total Akt (totAkt) and calnexin (cnx) as loading controls and revealed for quantification by Odissey Imaging System. Quantification of western blot analysis is reported as an average of four independent experiments, and represented as ratio pAkt/totAkt, assigning wild type as 1±s.e.m. p-Akt was significantly increased in vimentin-null nerves (***P=0.0004; n=4). (**B**) Homogenates of sciatic nerve lysates from P20 wild type and vimentin null. Blots were probed for phospho-ERBB2 (pERBB2) and total ERBB2 (totERBB2), and calnexin as loading control and revealed by Odissey. Quantification of western blot analysis is reported as an average of three independent experiments, and represented as a ratio of phospho-ERBB2/ERBB2 or phospho-ERBB2/cnx, assigning wild type as 1±s.e.m. Although the ratio of phospho-ERBB2/ERBB2 did not show differences, the amount of phospho-ERBB2 was significantly increased in vimentin-null when compared with wild-type nerves (*P=0.02; n=3).

leads to an increase of axonal NRG1 type III (Fig. 6G-I). Furthermore, the percentage of the number of axons per Remak bundle (Fig. 6H), and the percentage of axons per Schwann cell pocket (Fig. 6I) were significantly reduced in *Vim*$^{-/-}$ *Nrg1*$^{+/-}$ nerves when compared with *Nrg1* haploinsufficient mice. All these results confirmed that vimentin modulates NRG1 type III levels in neurons and thus regulates the amount of myelin thickness in Schwann cells.

Vimentin and TACE cooperate as negative regulators of myelination

NRG1 type III levels are regulated by BACE1 and TACE secretases (Hu et al., 2006; La Marca et al., 2011; Willem et al., 2006). BACE1 cleavage of NRG1 positively regulates myelination; however, TACE sheds the active form of NRG1 to an inactive form, thus acting as a negative regulator of myelination. Hence, genetic inactivation of TACE results in peripheral nerve hypermyelination (La Marca et al., 2011). As vimentin-null mice phenocopy hypermyelination in TACE-null mice, and both act through NRG1 type III, we investigated whether vimentin and TACE might act synergistically to induce hypermyelination. *Vim*$^{+/-}$ and *Tace*$^{+/-}$ mouse nerves are normally myelinated (La Marca et al., 2011) (data not shown). Of note, double heterozygous *Vim*$^{+/-}$ *Tace*$^{+/-}$ are hypermyelinated in the PNS (Fig. 7A-C) and mean g-ratio significantly reduced in double heterozygous *Vim*$^{+/-}$ *Tace*$^{+/-}$ mice (*Vim*$^{+/-}$ *Tace*$^{+/-}$ 0.67±0.02 versus *Vim*$^{+/+}$ *Tace*$^{+/+}$ 0.71±0.02; P<0.001; n=548 fibers per genotype, three mice per genotype). Western blot analysis confirmed a significant increase in MBP levels in double heterozygous mice (Fig. 7E). Morphometric analysis of double heterozygous *Vim*$^{+/-}$ *Tace*$^{+/-}$ nerves did not show significant differences of fiber type distribution when compared with controls (Fig. 7D). These results provide strong evidence that vimentin genetically interacts with TACE to modulate levels of NRG1 type III and myelination.

Conclusions

In this study, we describe for the first time the role of a cytoskeleton constituent, IF vimentin, as a negative regulator of myelination. We show that neuronal vimentin regulates Schwann cell myelin thickness by modulating levels of NRG1 type III. Furthermore, we show that vimentin genetically interacts with TACE to modulate myelin thickness.

The control of myelin thickness is fundamental for proper propagation of electrical impulses along the axons and for preservation of their integrity. In fact, peripheral neuropathies are characterized by abnormal myelin thickness, which may secondarily result in axon damage. Understanding processes that control myelin formation is therefore crucial to develop new potential treatments for peripheral neuropathies and dysmyelinating disorders. We report here that vimentin plays a role as a negative regulator of myelination. Different strategies in vivo and in vitro showed that loss of vimentin results in increased myelin thickness through a Schwann cell extrinsic mechanism. Hypermyelination is the consequence of vimentin depletion in neurons, as wild-type Schwann cells still hypermyelinate when co-cultured with vimentin-null neurons. Instead, hypermyelination did not occur in the reverse experiment. Of note, vimentin knockdown in Schwann cells caused hypomyelination rather then hypermyelination. This phenomenon may be the consequence of the acute downregulation of vimentin in Schwann cells, as it was restricted to in vitro studies and not detected in vivo in vimentin-null mice. It is thus possible to speculate that vimentin might have an additional role in earlier stages of PNS development, when Schwann cells have to contact the axons and elongate prior to myelination. Vimentin-null mice do not show any developmental-related phenotype, likely because of compensatory/redundant mechanisms by other intermediate filaments (such as nestin and GFAP) (Jessen and Mirsky, 2005) at earlier stage of development.

Although this is the first report of an intermediate filament being involved in the regulation of myelination, a role for cytoskeletal proteins in the control of myelination is now emerging. A recent study reported the Schwann cell-autonomous role of spectrin in controlling myelination, as spectrin downregulation impairs myelin formation (Susuki et al., 2011).

The mechanism that regulates myelin formation is not completely understood. Schwann cell fate and the amount of myelination is determined by levels of axonal NRG1 type III (Michailov et al., 2004; Taveggia et al., 2005). NRG1 binding to the ERBB2/3 receptor on Schwann cell plasma membrane activates the PI3-kinase pathway, resulting in myelination (Ogata et al., 2004; Taveggia et al., 2005). In our study, we observed increased expression of NRG1 type III in vimentin-null neurons (by both immunohistochemistry and western blot), increased levels of phospho-ERBB2, and of phospho-Akt, the key effector of the PI3-kinase pathway. Hence, vimentin in neurons participates in modulating NRG1 type III expression, and consequently myelin formation. Accordingly, rescue experiment aimed at reducing levels of NRG1 type III in vimentin-null

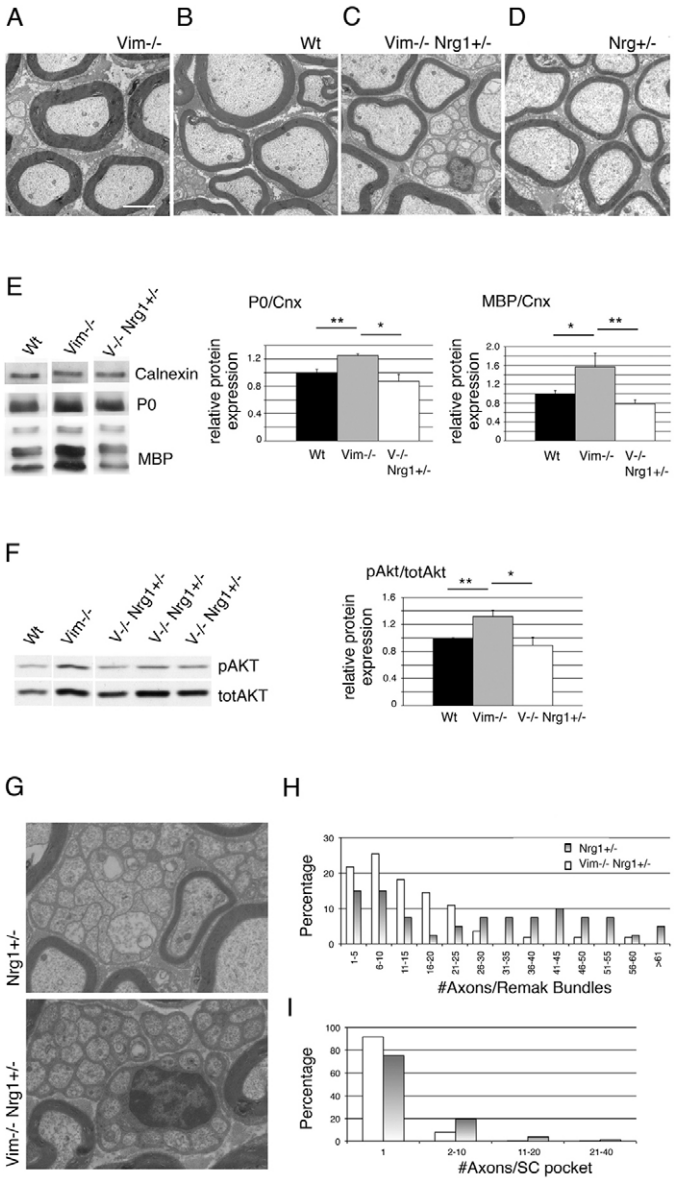

Fig. 6. Reduced levels of type III NRG1 rescue hypermyelination in vimentin-null mice. (**A-D**) Electron micrographs of sciatic nerve from P60 *Vim*$^{-/-}$ (A), wild-type (B), *Vim*$^{-/-}$ *Nrg1*$^{+/-}$ (C) and *Nrg1*$^{+/-}$ (D) mice. Increased myelin thickness observed in *Vim*$^{-/-}$ mice is rescued by 50%, reducing NRG1 levels in double *Vim*$^{-/-}$ *Nrg1*$^{+/-}$ mice. (**E**) Homogenate of sciatic nerve lysates from P60 wild-type, *Vim*$^{-/-}$ and *Vim*$^{-/-}$ *Nrg1*$^{+/-}$ mice. Calnexin is used as loading control. Quantification of western blot analysis is reported as an average of three independent experiments, and represented as ratio P0/calnexin and MBP/calnexin, assigning wild type as 1±s.e.m. A significant increased amount of P0 is observed in *Vim*$^{-/-}$ homogenate when compared with wild type (**P=0.01; n=3), which is significantly reduced towards normal levels in *Vim*$^{-/-}$ *Nrg1*$^{+/-}$ mice (*P=0.04; n=3). Similarly, a significant increased amount of MBP is observed in vimentin null when compared with wild type (*P=0.04; n=3), which is significantly reduced towards normal levels in *Vim*$^{-/-}$ *Nrg1*$^{+/-}$ mice (**P=0.01; n=3. (**F**) Homogenate of sciatic nerve lysates from 2-month-old wild-type, *Vim*$^{-/-}$ and *Vim*$^{-/-}$ *Nrg1*$^{+/-}$ mice. Quantification of western blot analysis is reported as an average of three independent experiments, and represented as ratio phospho-Akt/tot Akt, assigning wild type as 1±s.e.m. Levels of phospho-Akt are significantly increased in *Vim*$^{-/-}$ mice when compared with wild type (**P=0.01; n=3), and are significantly reduced towards normal levels in *Vim*$^{-/-}$ *Nrg1*$^{+/-}$ mice (*P=0.04; n=3). (**G**) Electron micrographs of sciatic nerve from 2-month-old *Nrg1*$^{+/-}$ and vimentin-null *Nrg1*$^{+/-}$ mice showing Remak bundles. As previously reported (Taveggia et al., 2005), Remak bundles in *Nrg1*$^{+/-}$ nerves present altered axonal segregation, as they have an increased number of axons and many axons that directly appose each other without intervening Schwann cell processes. When levels of NRG1 are elevated in *Vim*$^{-/-}$ *Nrg1*$^{+/-}$, this defect is almost rescued. (**H**) Histogram showing the percentage of the number of axons per Remak bundle, binned into separate groups, as a percentage of the total axons in *Nrg1*$^{+/-}$ and *Vim*$^{-/-}$ *Nrg1*$^{+/-}$ sciatic nerves (n=100 bundles for each genotype, two mice per genotype). In *Vim*$^{-/-}$ *Nrg1*$^{+/-}$, the number of axons per Remak bundle is reduced when compared with *Nrg1*$^{+/-}$ mice, similar to what described in wild-type nerves (Taveggia et al., 2005). The difference in fiber type distribution in the two groups was significant (χ^2, P<0.001). (**I**) The percentage of axons in Schwann cell pockets in Remak bundles were binned into four categories and counted in *Nrg1*$^{+/-}$ and *Vim*$^{-/-}$ *Nrg1*$^{+/-}$ sciatic nerves (n=700 unmyelinated axons for each genotype, two mice per genotype). Although many axons are present per Schwann cell pockets in *Nrg1*$^{+/-}$ nerves, as previously described (Taveggia, 2005), when the level of NRG1 is elevated in double heterozygous mice (*Vim*$^{-/-}$ *Nrg1*$^{+/-}$), almost all axons are present in individual Schwann cell pocket. Differences between the two groups were significant (χ^2; P=0.01). Scale

nerves resulted in reduced myelin thickness, and reduced levels of myelin proteins and phospho-Akt. Our findings mostly recapitulate what previously observed in other hypermyelinating mutants in which NRG1 type III or the pathway it activates, is increased, as in NRG1-overexpressing mice, in Tace conditional knockout mice and in *Pten*-null mice (Goebbels et al., 2010; La Marca et al., 2011; Michailov et al., 2004). The only difference was that increased amount of NRG1 signaling in vimentin-null mice was not sufficient to induce myelination of unmyelinated axons, as we did not find myelinated fibers smaller that 1.0 µm. Ectopic myelination in the presence of myelinated axons smaller than 1.0 µm was observed in *Tace*Fl/Fl Hb9Cre and *Pten*-null mutant mice, but was not investigated in NRG1-overexpressing mice. However, in vimentin-null mice the increase of hypermyelination is not as pronounced as that observed in other hypermyelinating models, possibly explaining the lack of ectopic myelination in these mutants.

In vitro findings not only confirmed that loss of vimentin in neurons results in increased myelin thickness, but also showed an increase in the number of myelin internodes. These data may suggest that ablation of neuronal vimentin is sufficient to initiate myelination also in vivo. Nevertheless, we did not find in vivo that myelination was temporally anticipated nor that small unmyelinated fibers became myelinated in vimentin-null mice. Initiation of myelination is a complex event in which vimentin could participate as a part of a composite machinery. Although the in vitro myelination co-culture system is a valid and well-established system that recapitulates the main events occurring in myelination, this is clearly less complex than the in vivo situation. Thus, it is possible that in vivo vimentin is mainly implicated in controlling myelin thickness and is not sufficient to dictate initiation of myelination, which could be controlled by other mechanisms also acting on NRG1 type III.

Increased NRG1 type III levels may be the consequence of (1) increased synthesis, (2) increased transport along the axons and (3) increased activation/reduced inactivation. How NRG1 is synthesized and transported along the axon to the plasma membrane is not known. It seems unlikely that vimentin and NRG1 type III interact, as loss of vimentin results in hypermyelination, whereas loss of NRG1 type III in hypomyelination. However,

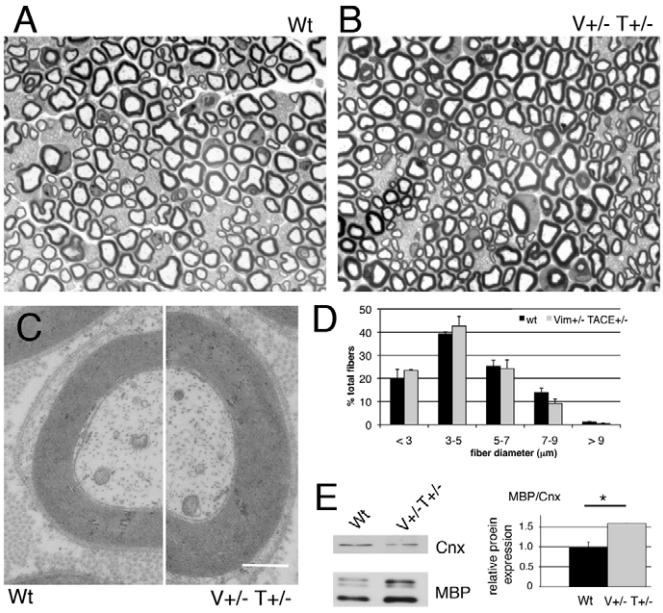

bar: 1.5 μm in A-D; and 4 μm in G.

Fig. 7. Vimentin and TACE interact to induce increased myelin thickness. (**A**,**B**) Semi-thin sections of sciatic nerve from 2-month-old wild-type (A) and double heterozygous *Vim*$^{+/-}$ *Tace*$^{+/-}$ (B) mice. Double heterozygous mice show a consisting number of fibers with increased myelin thickness. (**C**) Electron micrograph showing a single nerve fiber hypermyelinated in *Vim*$^{+/-}$ *Tace*$^{+/-}$ mouse (right) when compared with wild type (left). (**D**) Morphometric analysis did not show significant differences in terms of fiber size and density between wild-type and double heterozygous *Vim*$^{+/-}$ *Tace*$^{+/-}$ mice. (**E**) Sciatic nerve homogenate from P60 wild-type and *Vim*$^{+/-}$ *Tace*$^{+/-}$ mice blotted with anti-P0 antibody, and calnexin for loading control, showing increased levels of MBP. Quantification of western blot analysis is reported as an average of three independent experiments, and represented as ratio MBP/calnexin, assigning wild type as 1±s.e.m.: wild type 1±0.1 versus *Vim*$^{+/-}$ *Tace*$^{+/-}$ 1.59±0.002; **P*=0.03; *n*=3. Scale bar: 20 μm in A,B; 2 μm in C.

NRG1 type III is processed by endopeptidasis to regulate its activity. In fact, the α-secretase TACE sheds NRG1 type III and inactivates its function (Horiuchi et al., 2005; La Marca et al., 2011). Interestingly, genetic inactivation of TACE resulted in peripheral nerve hypermyelination as in vimentin-null mice (La Marca et al., 2011), suggesting that these molecules could belong to the same pathway that modulates myelination. In agreement, in a classical genetic experiment, we observed that *Vim*$^{+/-}$ *Tace*$^{+/-}$ nerves were hypermyelinated, thus phenocopying single gene inactivation in homozygousity, whereas both *Vim*$^{+/-}$ or *Tace*$^{+/-}$ heterozygous mice were normally myelinated.

Recent reports expanded the potential role of vimentin as a dynamic and mobile scaffold for localization and long-distance transport of soluble molecules. Vimentin can move bi-directionally on microtubules, towards plus ends in association with kinesin (Prahlad et al., 1998), and towards minus ends in association with dynein (Helfand et al., 2002). In neurons, vimentin was shown to regulate the axonal transport of phosphorylated MAP kinesis after injury (Perlson et al., 2005). It is tempting to speculate that vimentin regulates NRG1 levels by presenting TACE at the site of its protease activity. However, whether and how vimentin is involved in the transport of NRG1-associated sheddases will need further investigation.

In conclusion, we describe a previously uncharacterized mechanism that controls peripheral nerve myelination during development by modulating the NRG1 type III signaling pathway. For the first time, intermediate filaments are shown to be directly involved in controlling myelination and we provide evidence that vimentin and TACE act on the same pathway to regulate myelination. Thus, our study provides a new opportunity for understanding mechanisms that may regulate NRG1 type III signaling in axons, and new potential targets for therapeutic intervention.

Acknowledgements
The authors are grateful to Charles Babinet and Albee Messing for providing vimentin null mice; to Larry Wrabetz, Laura Feltri for discussion of data; and to ALEMBIC for the use of the electron microscope.

Funding
This work was supported by grants from Telethon Italy Foundation [GGP08037 to S.C.P.; GPP10007 to S.C.P., C.T. and A.B.], Association Française contre les Myopathies (AFM) and ERA-Net for research programs on rare diseases (E-rare) to A.B. A.B. is a recipient of a Telethon Career Award.

Competing interests statement
The authors declare no competing financial interests.

References

Belecky-Adams, T., Holmes, M., Shan, Y., Tedesco, C. S., Mascari, C., Kaul, A., Wight, D. C., Morris, R. E., Sussman, M., Diamond, J. et al. (2003). An intact intermediate filament network is required for collateral sprouting of small diameter nerve fibers. *J. Neurosci.* **23**, 9312-9319.
Bolis, A., Coviello, S., Visigalli, I., Taveggia, C., Bachi, A., Chishti, A. H., Hanada, T., Quattrini, A., Previtali, S. C., Biffi, A. et al. (2009). Dlg1, Sec8, and Mtmr2 regulate membrane homeostasis in Schwann cell myelination. *J. Neurosci.* **29**, 8858-8870.
Cochard, P. and Paulin, D. (1984). Initial expression of neurofilaments and vimentin in the central and peripheral nervous system of the mouse embryo in vivo. *J. Neurosci.* **4**, 2080-2094.
Colucci-Guyon, E., Portier, M. M., Dunia, I., Paulin, D., Pournin, S. and Babinet, C. (1994). Mice lacking vimentin develop and reproduce without an obvious phenotype. *Cell* **79**, 679-694.
Coulombe, P. A. and Wong, P. (2004). Cytoplasmic intermediate filaments revealed as dynamic and multipurpose scaffolds. *Nat. Cell. Biol.* **6**, 699-706.
Eriksson, J. E., Dechat, T., Grin, B., Helfand, B., Mendez, M., Pallari, H. M. and Goldman, R. D. (2009). Introducing intermediate filaments: from discovery to disease. *J. Clin. Invest.* **119**, 1763-1771.
Fitzpatrick, V. D., Pisacane, P. I., Vandlen, R. L. and Sliwkowski, M. X. (1998). Formation of a high affinity heregulin binding site using the soluble extracellular domains of ErbB2 with ErbB3 or ErbB4. *FEBS Lett.* **431**, 102-106.
Friede, R. L. and Bischhausen, R. (1980). The precise geometry of large internodes. *J. Neurol. Sci.* **48**, 367-381.
Goebbels, S., Oltrogge, J. H., Kemper, R., Heilmann, I., Bormuth, I., Wolfer, S., Wichert, S. P., Mobius, W., Liu, X., Lappe-Siefke, C. et al. (2010). Elevated phosphatidylinositol 3,4,5-trisphosphate in glia triggers cell-autonomous membrane wrapping and myelination. *J. Neurosci.* **30**, 8953-8964.
Helfand, B. T., Mikami, A., Vallee, R. B. and Goldman, R. D. (2002). A requirement for cytoplasmic dynein and dynactin in intermediate filament network assembly and organization. *J. Cell Biol.* **157**, 795-806.
Horiuchi, K., Zhou, H. M., Kelly, K., Manova, K. and Blobel, C. P. (2005). Evaluation of the contributions of ADAMs 9, 12, 15, 17, and 19 to heart development and ectodomain shedding of neuregulins beta1 and beta2. *Dev Biol.* **283**, 459-471.
Horiuchi, K., Kimura, T., Miyamoto, T., Takaishi, H., Okada, Y., Toyama, Y. and Blobel, C. P. (2007). Cutting edge: TNF-alpha-converting enzyme (TACE/ADAM17) inactivation in mouse myeloid cells prevents lethality from endotoxin shock. *J. Immunol.* **179**, 2686-2689.
Hu, X., Hicks, C. W., He, W., Wong, P., Macklin, W. B., Trapp, B. D. and Yan, R. (2006). Bace1 modulates myelination in the central and peripheral nervous system. *Nat. Neurosci* **9**, 1520-1525.
Jessen, K. R. and Mirsky, R. (1991). Schwann cell precursors and their development. *Glia* **4**, 185-194.
Jessen, K. R. and Mirsky, R. (2005). The origin and development of glial cells in peripheral nerves. *Nat. Rev. Neurosci.* **6**, 671-682.
Julien, J. P. (1999). Neurofilament functions in health and disease. *Curr. Opin. Neurobiol.* **9**, 554-560.

La Marca, R., Cerri, F., Horiuchi, K., Bachi, A., Feltri, M. L., Wrabetz, L., Blobel, C. P., Quattrini, A., Salzer, J. L. and Taveggia, C. (2011). TACE (ADAM17) inhibits Schwann cell myelination. *Nat. Neurosci.* **14**, 857-865.
McCall, M. A., Gregg, R. G., Behringer, R. R., Brenner, M., Delaney, C. L., Galbreath, E. J., Zhang, C. L., Pearce, R. A., Chiu, S. Y. and Messing, A. (1996). Targeted deletion in astrocyte intermediate filament (Gfap) alters neuronal physiology. *Proc. Natl. Acad. Sci. USA* **93**, 6361-6366.
Michailov, G. V., Sereda, M. W., Brinkmann, B. G., Fischer, T. M., Haug, B., Birchmeier, C., Role, L., Lai, C., Schwab, M. H. and Nave, K. A. (2004). Axonal neuregulin-1 regulates myelin sheath thickness. *Science* **304**, 700-703.
Neuberger, T. J. and Cornbrooks, C. J. (1989). Transient modulation of Schwann cell antigens after peripheral nerve transection and subsequent regeneration. *J. Neurocytol.* **18**, 695-710.
Ogata, T., Iijima, S., Hoshikawa, S., Miura, T., Yamamoto, S., Oda, H., Nakamura, K. and Tanaka, S. (2004). Opposing extracellular signal-regulated kinase and Akt pathways control Schwann cell myelination. *J. Neurosci.* **24**, 6724-6732.
Perlson, E., Hanz, S., Ben-Yaakov, K., Segal-Ruder, Y., Seger, R. and Fainzilber, M. (2005). Vimentin-dependent spatial translocation of an activated MAP kinase in injured nerve. *Neuron* **45**, 715-726.
Prahlad, V., Yoon, M., Moir, R. D., Vale, R. D. and Goldman, R. D. (1998). Rapid movements of vimentin on microtubule tracks: kinesin-dependent assembly of intermediate filament networks. *J. Cell Biol.* **143**, 159-170.
Previtali, S. C., Quattrini, A., Fasolini, M., Panzeri, M. C., Villa, A., Filbin, M. T., Li, W., Chiu, S. Y., Messing, A., Wrabetz, L. et al. (2000). Epitope-tagged P(0) glycoprotein causes Charcot-Marie-Tooth-like neuropathy in transgenic mice. *J. Cell Biol.* **151**, 1035-1046.
Susuki, K., Raphael, A. R., Ogawa, Y., Stankewich, M. C., Peles, E., Talbot, W. S. and Rasband, M. N. (2011). Schwann cell spectrins modulate peripheral nerve myelination. *Proc. Natl. Acad. Sci. USA* **108**, 8009-8014.
Suter, U. and Scherer, S. S. (2003). Disease mechanisms in inherited neuropathies. *Nat. Rev. Neurosci.* **4**, 714-726.
Taveggia, C., Zanazzi, G., Petrylak, A., Yano, H., Rosenbluth, J., Einheber, S., Xu, X., Esper, R. M., Loeb, J. A., Shrager, P. et al. (2005). Neuregulin-1 type III determines the ensheathment fate of axons. *Neuron* **47**, 681-694.
Triolo, D., Dina, G., Lorenzetti, I., Malaguti, M., Morana, P., Del Carro, U., Comi, G., Messing, A., Quattrini, A. and Previtali, S. C. (2006). Loss of glial fibrillary acidic protein (GFAP) impairs Schwann cell proliferation and delays nerve regeneration after damage. *J. Cell Sci.* **119**, 3981-3993.
Willem, M., Garratt, A. N., Novak, B., Citron, M., Kaufmann, S., Rittger, A., DeStrooper, B., Saftig, P., Birchmeier, C. and Haass, C. (2006). Control of peripheral nerve myelination by the beta-secretase BACE1. *Science* **314**, 664-666.
Wolpowitz, D., Mason, T. B., Dietrich, P., Mendelsohn, M., Talmage, D. A. and Role, L. W. (2000). Cysteine-rich domain isoforms of the neuregulin-1 gene are required for maintenance of peripheral synapses. *Neuron* **25**, 79-91.